Review

Metallosurfactants of bioinorganic interest: Coordination-induced self assembly

Tate Owen [1], Alison Butler[*]

Department of Chemistry & Biochemistry, University of California, Santa Barbara, CA 93106-9510, United States

Contents

ARTICLE INFO

ABSTRACT

This review covers selected surfactant ligands that undergo a change in aggregate morphology upon coordination of a metal ion, with a particular focus on coordination-induced micelle-to-vesicle transitions. The surfactants include microbially produced amphiphilic siderophores, as well as synthetic amphiphilic ligands. The mechanism of the metal-induced phase change is considered in light of the coordination chemistry of the metal ions, the nature of the ligands, and changes in molecular geometry that result from metal coordination. Of particular interest are biologically produced amphiphiles that coordinate transition metal ions and amphiphilic ligands of relevance to bioinorganic chemistry.

© 2010 Elsevier B.V. All rights reserved.

1. Introduction

Metallosurfactants are amphiphilic compounds that coordinate metal ions. Most metal-coordinating groups are inherently polar and comprise the hydrophilic headgroup of the surfactant. While their amphiphilic nature makes them attractive candidates for the assembly of nano-scale, metal-containing colloids, the headgroup ligand can impart a rich metal-coordination chemistry that can be used to tune the nature of the self-assembled structures. Metallosurfactants have been reviewed recently from a number of different perspectives, including metallomicelles [1,2], supramolecular aggregates of lipophilic Gd(III)-MRI contrast agents [3], metalloaggregates for catalysis, transport and sensing [4,5], nanoscale molecular containers for fluorescent sensors [6], and for metal extraction strategies [7]. Because the metal-cation is generally located at the hydrophilic–hydrophobic interface of the colloid, metallosurfactants are attractive as catalysts to react with either hydrophilic or hydrophobic substrates [8,9].

The focus of this review is on metallosurfactants that undergo a micelle to vesicle transition upon metal coordination. The phase that is adopted by a particular surfactant is strongly influenced by that surfactant's molecular geometry (i.e., headgroup-area-to-lipid-tail-volume ratio) and electrostatic charge [10]. Coordination of a metal can change a surfactant's geometry and/or electrostatic charge and thus induce a change in aggregate morphology.

* Corresponding author. Tel.: +1 805 893 8178.
  E-mail address: butler@chem.ucsb.edu (A. Butler).
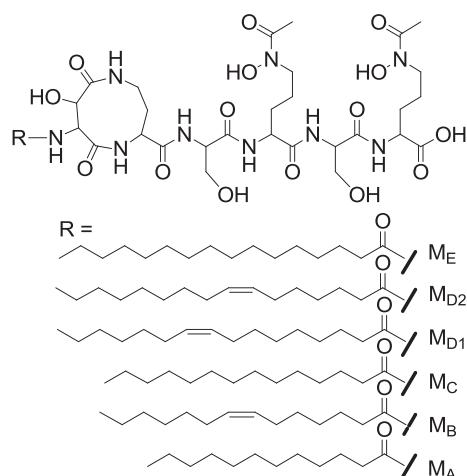[1] Current address: Genalyte Inc, San Diego, CA 92037.

Fig. 1. Marinobactins A–E. Fe(III) coordination occurs via the bidentate hydroxamate and hydroxamide groups [11].

Fig. 2. Schematic of a composite, dual-tailed surfactant that may be formed when "excess" Fe(III) bridges two Fe(III)-ME headgroups [14]. Relative to a single-tailed surfactant, a dual-tailed surfactant would have a smaller headgroup area: tail volume ratio that may favor vesicle formation [10].

Specifically, a metal cation can bridge multiple surfactant headgroups. Bridging multiple headgroups with a metal cation can either draw the headgroups closer together, or push them apart, depending on the chemical structure of the surfactant, such that an aggregate of lesser or greater curvature is preferred, respectively. This review summarizes selected surfactants that exhibit this kind of metal-dependent phase behavior. The phase behavior of these surfactants is discussed in terms of coordination chemistry and surfactant self-assembly. Of particular interest are biologically produced amphiphiles that coordinate transition metal ions and amphiphilic ligands of relevance to bioinorganic chemistry.

2. Amphiphilic siderophores

Marinobactins A–E (M_A–M_E, Fig. 1) are a suite of amphiphilic siderophores produced by a marine bacterium [11]. Siderophores are a class of compounds produced by bacteria for the purpose of obtaining iron as a nutrient [12]. The peptide headgroup of the marinobactins is comprised of a mixture of D and L amino acids which coordinate Fe(III) through two hydroxamic acid moieties and an α-hydroxylamide functionality [11,13]. M_D and M_E, which have the longest fatty acid tails (C16:1 and C16:0, respectively), are produced in the greatest quantity when DS40M6 is grown in culture at room temperature.

The critical micelle concentration (CMC) of apo-M_E (i.e., M_E that is not coordinated to Fe(III)) and Fe(III)-M_E are relatively low at ~50 and ~75 μM, respectively [11]. At concentrations above the CMC, small-angle neutron scattering (SANS) data reveal that apo-M_E aggregates to form spherical micelles that decrease in diameter upon coordination of Fe(III) (~4.6 nm and ~3.5 nm in diameter, respectively) [14]. The decrease in micelle diameter of Fe(III)-M_E is attributed to an increase in the head-group area relative to the lipid tail volume [10]. In the presence of excess Fe(III) (i.e., 0.1–2.0 equiv. Fe(III) per equiv. of Fe(III)-M_E), SANS data show a decrease in the micelle population and a concomitant increase in the vesicle population [14]. The vesicles are ~200 nm in diameter as measured by dynamic light scattering (DLS). We have hypothesized that the "excess" Fe(III) induces vesicle formation by bridging the terminal carboxylate moieties of two or three Fe(III)-M_E headgroups, thus pulling them closer together such that formation of a vesicular aggregate is favored (Fig. 2).

Other metals can be substituted for the "excess" iron to induce the Fe(III)-marinobactins to undergo the micelle-to-vesicle phase transition. For example, the addition of Zn(II), Cd(II), or La(III) to Fe(III)-M_E induces a micelle to multilamellar vesicle transition [15].
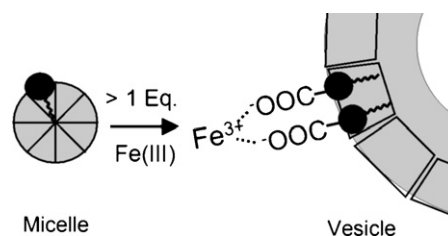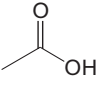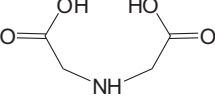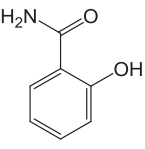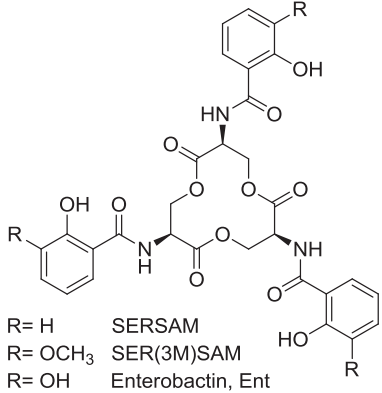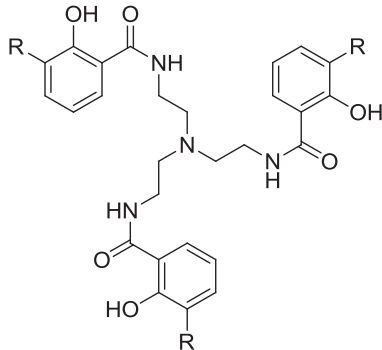
The vesicles can be disrupted by the addition of EDTA, in a process that leaves intact the Fe(III)-marinobactin moiety (that is Fe(III) coordinated by the headgroup hydroxamate and α-hydroxyamide ligands); thus the EDTA out competes complexation of the "excess" Fe(III) or the Zn(II), Cd(II), or La(III) ions that induce the metal-to-vesicle transition. In contrast to Fe(III)-M_E, the addition of Zn(II) to apo-M_E results in precipitation; no evidence for vesicle formation is found, showing that coordination to Fe(III) is a prerequisite for Zn(II)-induced vesicle formation. Similar to the "excess" Fe(III)-induced micelle to vesicle transition, we hypothesize that Zn(II), Cd(II), and La(III) induce a phase change by coordinating the terminal carboxylate group of multiple Fe(III)-M_E headgroups. This hypothesis is corroborated by the coordination chemistry of these metal ions with carboxylate ligands. Specifically, the metals that induce a phase change (i.e., Zn(II), Cd(II), La(III), and Fe(III)) form 2:1 ligand/metal coordination complexes with carboxylic acids like acetic acid (Table 1 [16]).

Zn(II) and Cd(II) EXAFS of the Zn(II)- and Cd(II)-induced vesicles of Fe(III)-marinobactins is consistent with octahedral coordination by six light atom ligands in the first coordination shell. The two light atoms in the second coordination shell are consistent with two carboxylate ligands [17]. The Fe(III) EXAFS of these vesicles is also fully consistent with ligation by the two hydroxamates and the α-hydroxyamide of the marinobactin headgroup [17].

Analysis of the SANS data for the multilamellar vesicles is suggestive of a solvent-filled core that makes up a very small fraction (<1%) of the overall vesicle volume. A relatively small solvent filled core is consistent with the absence of a visible hollow vesicle core in the cryo-transmission electron microscopy (cryo-TEM, Fig. 3) images. Thus, both the SANS and cryo-TEM data suggest the vesicles have bilayers with a range of curvatures that extend nearly to the center of the vesicle as depicted in Fig. 4.

One of the defining characteristics of marine siderophores is the prevalence of suites of amphiphilic siderophores produced by marine bacteria (Fig. 5). These siderophores span a range of amphiphilicities, from quite hydrophobic to quite hydrophilic, depending on the number of amino acids in the head group relative to the number and chain length of the fatty acid appendages. The amphibactins with only four amino acids in the headgroup and predominantly C18 fatty acids are much more hydrophobic than the loihichelins with eight amino acids in the headgroup and C12–C14 fatty acids. The amphibactins are sufficiently hydrophobic that they remain associated with the bacterium, as opposed to being released into the growth medium, whereas the loihichelins are not associated with the bacterium during the isolation process. Similarly the ochrobactins with two fatty acid appendages are much more hydrophobic that the synechobactins with one fatty acid. In fact the ochrobactins remain associated with the bacterium after centrifugation of the culture medium. While only the self-assembly of the marinobactins has been reported to date, investigations of the amphiphilic properties of the other marine siderophores are in progress.

Table 1
Stability constants of metals with representative functional groups.

Ligand	Metal	Stability constant	References	Of relevance to
Acetic acid	Fe(III)	$\beta_2 = 1.3 \times 10^6$	[16]	Marinobactin E
		$\beta_3 = 5.0 \times 10^8$	[16]	Marinobactin E
	Cu(II)	$\beta_2 = 4.3 \times 10^3$	[16]	SDUC
	Zn(II)	$\beta_2 = 123$	[16]	Marinobactin E
	Cd(II)	$\beta_2 = 1.4 \times 10^3$	[16]	Marinobactin E
	La(III)	$\beta_2 = 1.3 \times 10^5$	[16]	Marinobactin E
Iminodiacetic acid	Co(II)	$\beta_2 = 1.9 \times 10^{19}$	[16]	SHIDA
	Ni(II)	$\beta_2 = 2.0 \times 10^{14}$	[16]	SHIDA
	Cu(II)	$K_1 = 4.3 \times 10^{10}$	[16]	SHIDA/SDUC
		$\beta_2 = 4.8 \times 10^{16}$		
Salicylamide	Fe$^{(III)}$(salicylamide)$_2$	$\beta_2 = 1.8 \times 10^{16}$	[22]	Catechol amphiles, L^a, L^b
Enterobactin and analogs	[Fe$^{(III)}$Ent]$^{3-}$	$K = 10^{49}$	[23]	Catechol amphiphile, L^T
	[Fe$^{(III)}$EntH$_3$]^0	$K = 10^{37.92}$	[23]	Catechol amphiphile, L^T
	[Fe$^{(III)}$SERSAM]	$K = 10^{39}$	[24]	Catechol amphiphile, L^T
	[Fe$^{(III)}$SER(3M)SAM]	$K = 10^{38}$	[24]	Catechol amphiphile, L^T
	[Fe$^{(III)}$TRENCAM]$^{3-}$	$K = 10^{39}$	[25]	Catechol amphiphile, L^T
	[Fe$^{(III)}$TRENSAM]	$K = 10^{25.34}$	[25]	Catechol amphiphile, L^T

R= H   SERSAM
R= OCH$_3$ SER(3M)SAM
R= OH   Enterobactin, Ent

R = H   TRENSAM
R = OH   TRENCAM

3. Catecholate amphiphilic ligands

To mimic some of the biological and physical properties of the amphiphilic marinobactin siderophores and because many siderophores contain catechol functional groups, Pierre et al. have synthesized a series of amphiphilic catechol compounds [26–29].

Two of these amphiphiles have a "monopodal" headgroup consisting of a single dihydroxybenzoate moiety appended by octylamine or dodecylamine (L^a and L^b, Fig. 6) [26], and a third consists of a sulfonated dihydroxybenzoate moiety appended by decylamine, L^{S10} [27]. A "tripodal" amphiphile is comprised of a tris-catechol headgroup appended by a C16 tail (L^T, Fig. 6).
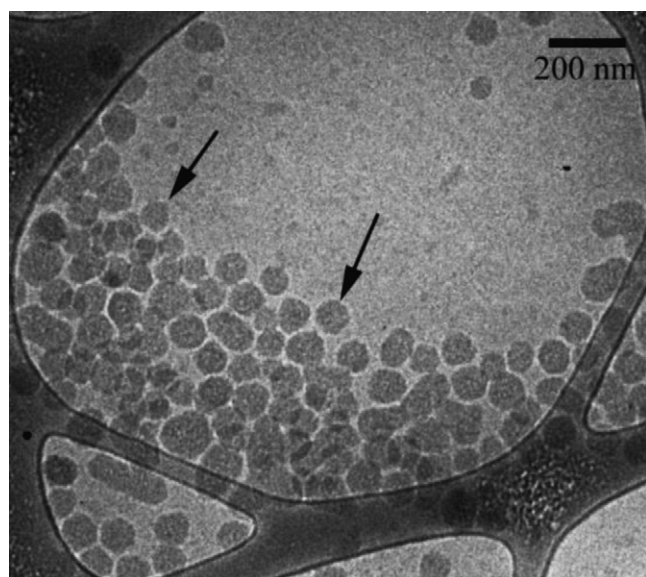
Fig. 3. Cryo-TEM micrograph of the Zn(II)-induced vesicles of Fe(III)-marinobactin [17]. Representative vesicles are indicated with arrows. The scale bar represents 200 nm.

Fig. 4. Schematic of Zn(II)-, Cd(II)-, or La(III)-induced micelle to multilamellar vesicle transition of the Fe(III)-marinobactins [17].

The CMC of the apo amphiphiles and the ferric complexes of L^a, L^b and L^T are <10^{-5} M at about neutral pH [26,27]. Cryo-TEM micrographs of the Fe(III)-complexes reveal the Fe(III)-amphiphiles form solid particles ~100–200 nm in diameter that resemble "filled" vesicles (Fig. 7a and b). In contrast, the apo-ligands form only micelles [26]. In the case of the monopodal catecholate ligands, the $[Fe(LH)_2]^+$ species would have two fatty acid tails and thus may have a predisposition to form vesicles over the single-tailed apo-ligand because of the expected change in shape from a conical apo-monopodal surfactant to a more cylindrically shaped dual tail complex (e.g., Fig. 7c) [10]. Based on the UV–vis spectra and potentiometric titration data, the speciation of the Fe(III) complexes of L^a and L^b fit best to $Fe(L^{a,b}H_2)^+$, with bis-salicylate coordination at the Fe(III)-center (Figs. 6 and 7c). Formation of a 2:1 ligand:metal species seems reasonable given that salicylamide forms a 2:1 com-
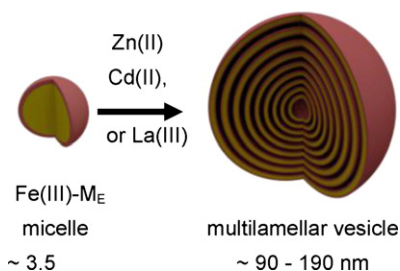
plex with Fe(III) with appreciable affinity, at β_2 1.8×10^{16} (Table 1 [22]).

Fe(III) coordination to L^T forms a 1:1 complex, signifying different characteristics of the Fe(III)-induced vesicle formation for Fe(III)-L^T because of the single fatty acid tail relative to the dual tailed Fe(III)-complexes of L^a and L^b. The predominant species in solution are $[Fe(L^TH)]^{2-}$ and $[Fe(L^TH_2)]^-$, suggestive of mixed salicylate and catecholate coordination, and consistent with the UV–vis spectrum [26]. The ferric stability constant for tris catecholate coordination in the siderophore enterobactin, Fe(III)Ent^{3-}, is quite large, at 10^{49} [23], as well as for the tripodal catecholate ligand, TREN-CAM, 10^{39} (Table 1 [25]). However, in the triprotonated derivative of tris catecholate ligands, such as $[Fe(III)-(H_3Ent)]^0$, the stability constant drops to $10^{37.92}$ consistent with tris-salicylate coordination, which is the only mode of coordination for Fe(III)-SERSAM (K, 10^{39}) [24], Fe(III)-SER(3 M)SAM (K, 10^{38}) [24], Fe(III)TRENSAM [25], and Fe(III)TREN(3 M)SAM [25] (Table 1).

The Gram-negative bacterium *Erwinia chrysanthemi* is even able to acquire iron from the Fe(III)-$(HL^a)_2^+$ complex [26]. Interestingly, lipidated catechols form a large class of natural products isolated from certain tree lacquer sap. In these compounds the alkyl tail (C15- and C17-saturated, as well as mono and di unsaturated cis double bonds at ω-7 and ω-9 positions, and ω-phenyl alkyl-(C10 or C12)-catechols) is appended to the catechol in a position ortho to one of the hydroxyl groups [30]. Moreover, the urushiols isolated from poison oak, poison ivy, and other plants is similarly, ortho catechol appended by C15 or C17 saturated alkyl
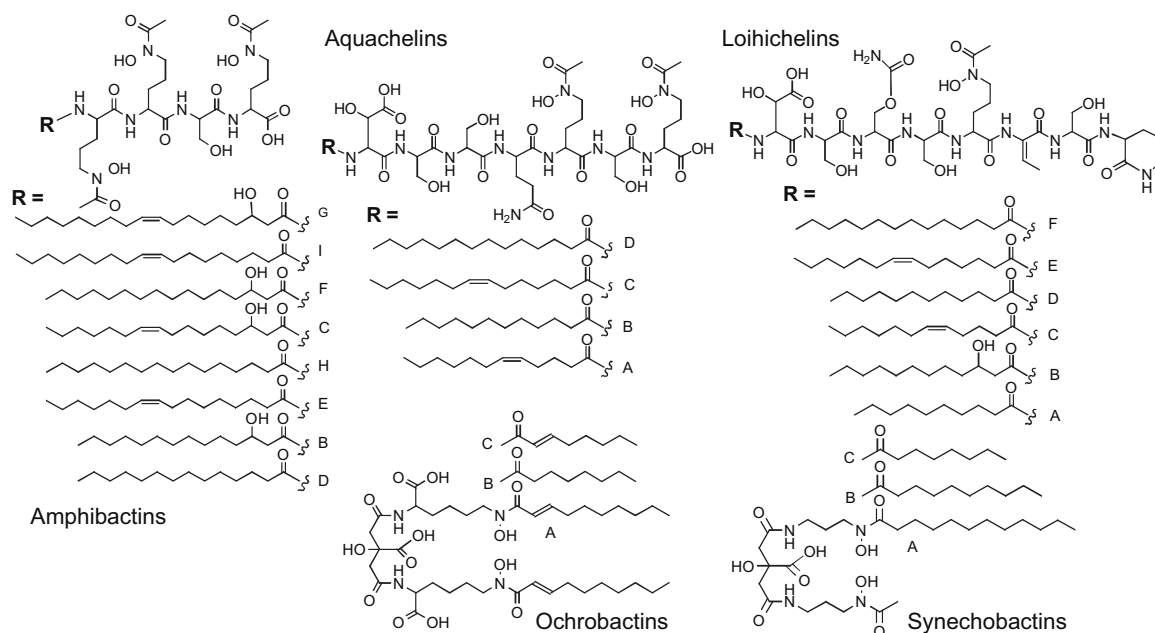

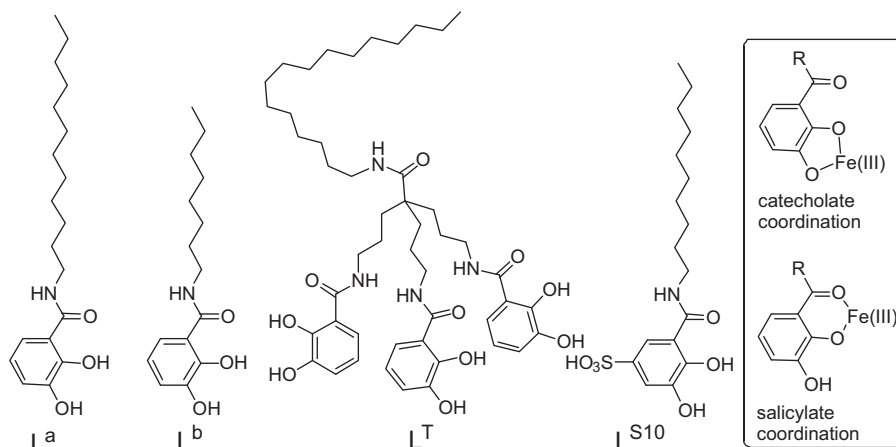**Fig. 5.** Other amphiphilic suites of marine siderophores [11,12,18–21].

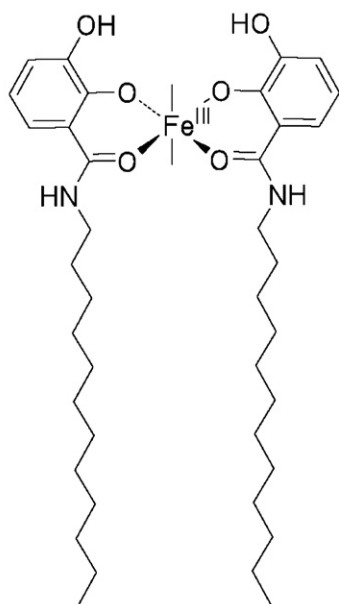**Fig. 6.** Monopodal and tripodal catechol amphiphiles [26,27].

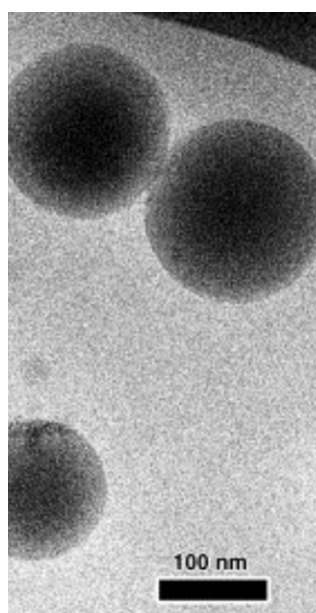**Fig. 7.** Left: cryo-TEM micrographs of 1 mM Fe(III)-(HL^a)$_2$$^+$ with 1% octanol (95/5, v/v H$_2$O/MeOH, pH 7.4); scale bar, 100 nm. Modified from Fig. 1 of Ref. [26]. Right: depiction of bis-salicylate coordination in Fe(III)-(HL^a)$_2$$^+$, the predominant species at pH 7.4.
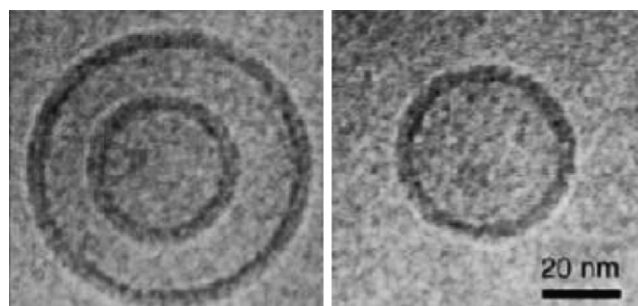

Fig. 8. Cryo-TEM of a ~3:1 ratio of Fe(III):L^{S10} after 8 days. Modified from Fig. 6 of Ref. [27].

tails that are saturated or unsaturated with up to three double bonds.

Sulfonation of the catechol substantially changes the amphiphilic properties of the monopodal catechol surfactants, significantly [27]. The CMC value of apo-L^{S10} is much higher, 1.2 mM, compared to cmc values of $<10^{-5}$ M for L^a, L^b and L^T, and ~1.45 mM for Fe(III) complexes of L^{S10}. The speciation of the Fe(III) complexes is also much more complicated, with variations in the ligand-to-Fe(III) ratio, the type of coordination (e.g., salicylate, catecholate), and nature of the self-assembled aggregation over

time and with pH [27]. Nevertheless, after 8 days, cryo-TEM shows vesicular structures, with a bilayer thickness that is the same as the micelle diameter (Fig. 8) [27].

Pierre et al. have also synthesized a series of ligand amphiphiles based on sulfonated 8-hydroxyquinoline, including the monopodal QS10 ligand appended by decylamine [29], which coordinates Fe(III) forming bis and tris ferric complexes. These new amphiphilic ligands are related to quinolobactin (8-hydroxy-4-methoxy-quinaldic acid; Fig. 9), a siderophore isolated from certain strains of *Pseudomonas fluorescens* [31]. The CMC value for apo-Q^{S10} seems to be quite large, exceeding the solubility of the ligand in water, although the tris ferric complex is in the μM range. [Fe(III)(Q^{S10})$_3$]$^{6-}$ aggregates into spheres of 100–200 nm in diameter, with unusual regions that have a higher iron density. Given the tris quinolinate coordination at neutral pH, thus a complex with three C10 acyl appendages, it will be interesting to learn what the molecular shape of this metalloamphiphile is.

4. Carboxylate surfactants

4.1. Dioctyl dicarboxylate

Sodium 4,8-dioctyl-3,9-dioxo-6-hydroxy-4,8-diaza-1,11-undecanedicarboxylate (SDUC) is a synthetic dicarboxylate
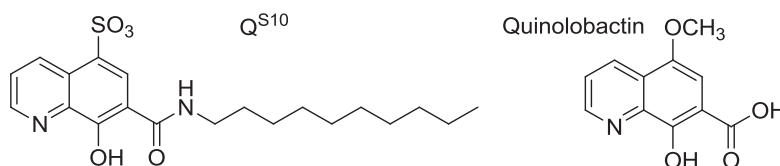

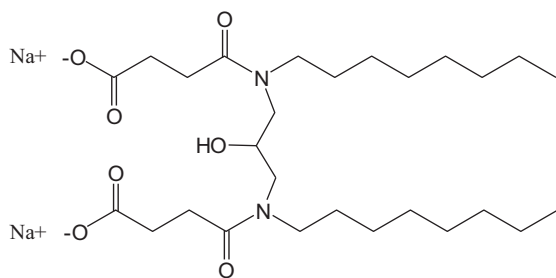**Fig. 9.** Structure of the amphiphilic sulfonated 8-hydroxyquinoline.

Fig. 10. Sodium 4,8-dioctyl-3,9-dioxo-6-hydroxy-4,8-diaza-1,11-undecane-dicarboxylate (SDUC), a gemini surfactant.

surfactant with two fatty acid appendages (Fig. 10). DLS measurements reveal that SDUC in aqueous solution forms a broad distribution of aggregates, with diameters ranging from ~2–400 nm when both carboxylates are deprotonated [32]. The authors suggest that the aggregates are micelles of varying sizes. In the presence of a small concentration of Cu(II) relative to SDUC (i.e., 0.02 mM Cu(II) to 2 mM SDUC at pH 12.0), vesicles are observed by negative staining TEM (Fig. 11), whereas in the absence of Cu(II) such recognizable aggregates were not identified. DLS measurements suggest the Cu(II)-containing solution consisted of both ~3 nm diameter micelles and ~140 nm diameter vesicles.

The authors proposed that SDUC forms vesicles because Cu(II) is coordinated by the carboxylate of multiple SDUC headgroups, thus neutralizing the electrostatic repulsion between headgroups and drawing the headgroups closer together as depicted in Fig. 12 [32]. While it is possible, as the authors suggest, that a carboxylate moiety from two different SDUC headgroups could coordinate Cu(II), it is also possible that both carboxylate moieties of a single SDUC ligand coordinate to a single Cu(II), as supported on thermodynamic grounds (Table 1). The stability constant, β_2 for Cu(acetate)$_2$ is 4.3×10^3 [16], whereas K_1 for Cu(iminodiacetate)^0 is 4.3×10^{10} and β_2 for Cu(iminodiacetate)$_2{}^{2-}$ is 4.8×10^{16} [16]. The relatively low stoichiometric ratio of Cu(II) to SDUC (i.e., 0.01 equivalents of Cu(II) per equivalent of SDUC) used to induce vesicle formation, was not discussed, although further potentiometric investigations
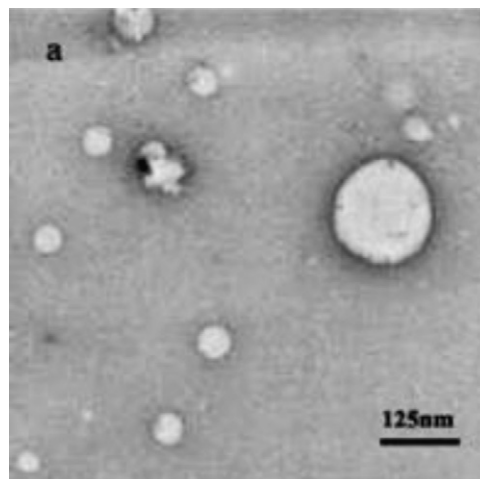

Fig. 11. TEM micrograph of vesicles of the Cu(II)-SDUC complex. Scale bar represents 125 nm.
Reproduced with permission [32].

could be useful to elucidate the nature of carboxylate coordination to Cu(II). X-ray diffraction (XRD) measurements on cast films of the SDUC vesicles yielded a bilayer thickness of 3.68 nm, which is roughly twice the molecular length of SDUC and suggests the lipid tails are not interdigitated in the vesicle bilayer [32].

4.2. Hexadecyliminodiacetate

Sodium hexadecyliminodiacetate (SHIDA, Fig. 13) is similar to SDUC (Fig. 10) in that the SHIDA headgroup contains two carboxylic acid moieties. In water, 10 mM SHIDA exists predominantly in the micellar state, consistent with the CMC value of about 1 mM. In the presence of 0.5 equiv. Cu(II), Co(II), or Ni(II), SHIDA rearranges to form vesicles as observed by TEM [33]. Based on the coordination chemistry of iminodiacetate (Table 1), the authors propose that two SHIDA headgroups coordinate to the divalent cation forming an octahedral complex at the Cu(II) and Co(II) centers, and a
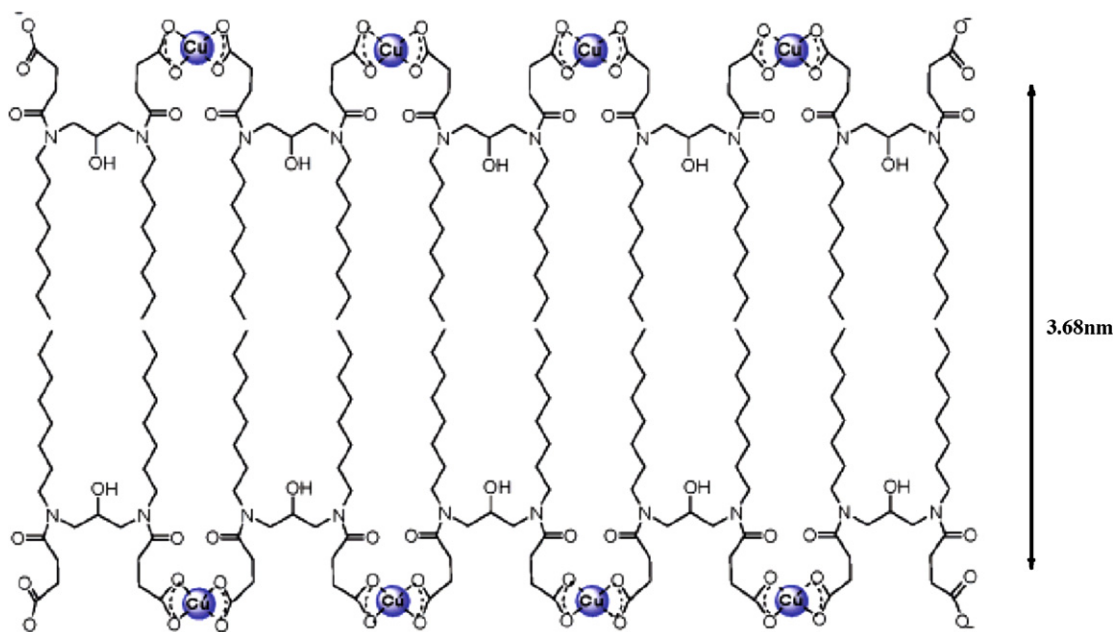

Fig. 12. Proposed Cu(II)-induced bilayer structure of the vesicles at pH 12.
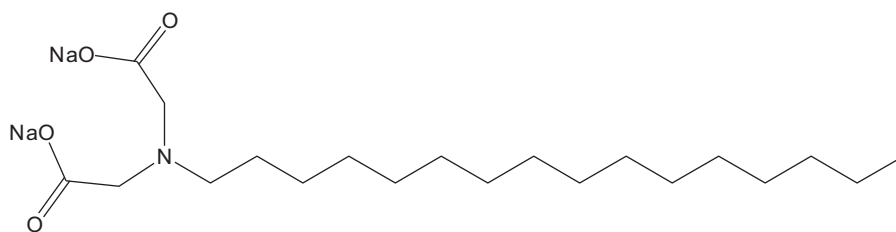Reproduced with permission [32].

Fig. 13. Sodium hexadecyliminodiacetate SHIDA [33].

square planar complex at the Ni(II) center, although octahedral coordination at Ni(II) is reasonable with N and O weak-field ligands. The effect of metal coordination thus draws the headgroups closer together forming a composite surfactant with two fatty acid appendages. The switch from a single fatty acid compound to a dual tailed surfactant would seem to favor bilayer vesicle formation (Fig. 14). XRD measurements on cast films of metal(II)-SHIDA vesicles resulted in a bilayer thickness of ~3–3.2 nm, which is slightly longer than the molecular length of SHIDA. This bilayer thickness suggests the lipid tails in the bilayers of SHIDA vesicles are interdigitated (Fig. 14). Interdigitating the lipid tails may allow more efficient packing of a single-tailed surfactant in a bilayer. In contrast, the dual tailed surfactant SDUC (Fig. 10) forms vesicles that do not appear to be interdigitated [32].

5. Octadecylamine

Octadecylamine ($C_{18}H_{37}NH_2$) is a cationic, single-tailed surfactant that forms micelles under acidic conditions. However, when 5 mM octadecylamine is sonicated in water with 0.5 equiv. of Ag^+, the surfactant forms vesicles as observed in TEM images [34]. The authors hypothesized that two octadecylamine headgroups coordinate a single Ag^+ ion to form a composite, dual-tailed surfactant that is then predisposed to form vesicles (Fig. 15) [34]. Methylamine coordinates Ag^+ as a 2:1 ligand/metal complex with a stability constant, β_2 of 5.3×10^6 [16], consistent with the proposed Ag(octadecylamine)$_2^+$ coordination. XRD profiles of cast films of the vesicles revealed a bilayer thickness of 4.55 nm, which is roughly twice the molecular length of octadecylamine, suggesting that the Ag(octadecylamine)$_2^+$ bilayers vesicles are not interdigitated, similar to the Cu(II)-induced bilayer formation of SDUC at pH 12 [32], but in contrast to the divalent metal complexes of SHIDA [33]. Although octadecylamine is a single-tailed surfactant, octadecylamine has a small headgroup and interdigitation may not be necessary for efficient packing of the surfactant tails into a vesicle bilayer.

Similar to the spontaneous micelle-to-vesicle phase change of octadecylamine in the presence of 0.5 equiv. Ag(I), and hexadecyliminodiacetate upon reaction with 0.5 equiv. Cu(II), Co(II) or Ni(II), n-undecylamine also undergoes a micelle-to-vesicle transition in the presence of Cu(II) at a 2:1 ratio of ligand:Cu(II) [35]. The vesicles that form spontaneously are polydisperse in size, ranging from 100 nm to 1000 nm, the latter of which is thought to result from fusion of vesicles. The phase behavior is rationalized on the Israelachvili packing model [10], going from a single alkyl chain before metal coordination to a dual tailed amphiphile in the Cu(II)-(undecylamine)$_2^{2+}$ complex.

6. Imidazolate surfactants

A surfactant with a bis-imidazole headgroup, 1,3-bis(1-imidazolyl)-2-propyl octadecanoate (Fig. 16) was synthesized to investigate the effect of metal coordination on its aggregation behavior [36]. The coordination chemistry of this dicephalic surfactant can be tuned by varying the pH, effecting chelate formation
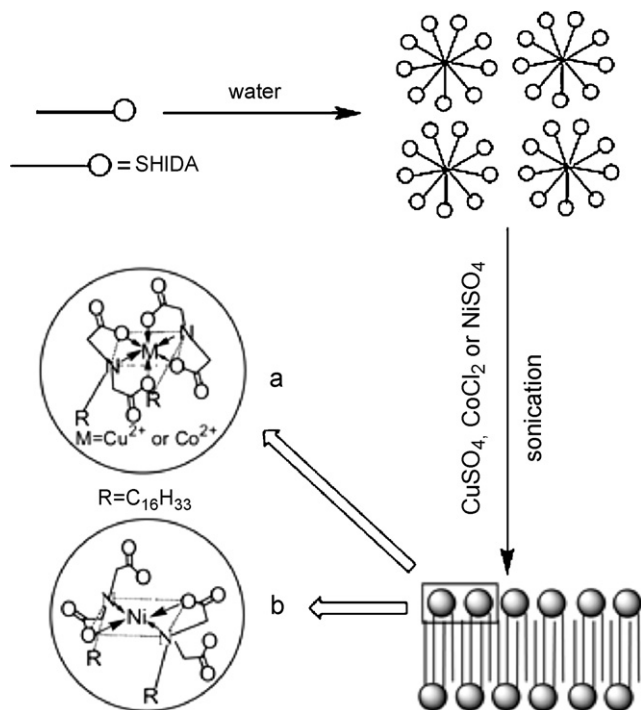

Fig. 14. Proposed micelle-to-bilayer transition of SHIDA upon coordination of Cu(II), Co(II), or Ni(II), depicting octahedral coordination at Cu(II) and Co(II) centers and square planar coordination at Ni(II).
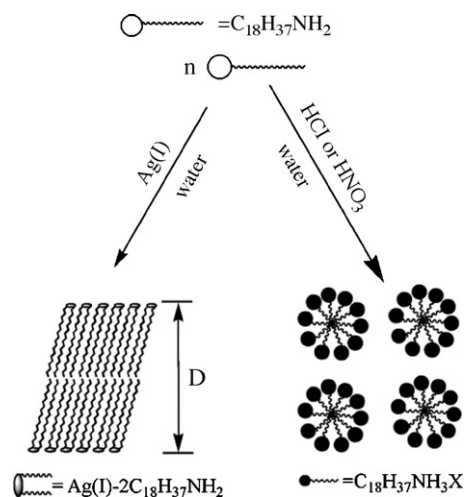Reproduced with permission [33].

Fig. 15. Schematic of micelle formation by octadecylamine in acidic conditions and bilayer formation upon coordination of Ag^+.
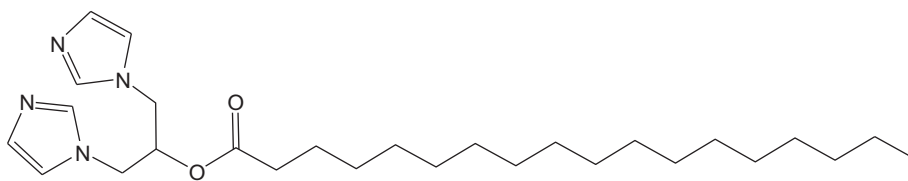Reproduced with permission from Ref. [34].

Fig. 16. The dicephalic bis-imidizole surfactant, 1,3-bis(1-imidazolyl)-2-propyl octadecanoate [36].

between one or more ligands and a single Cu(II) ion or polymerization in which the ligand coordinates to two Cu(II) ions and Cu(II) bridges two ligands, forming a networked array of ligand and metal. Freeze-fracture transmission electron microscopy (FF-TEM) reveals that at both pH 5.5 and 9.5 vesicles form that are ~50–250 nm in diameter. Differential scanning calorimetry (DSC) distinguishes the two forms, with a phase transition occurring at 15 °C for the pH 5.5 vesicles, and at 62 °C for the pH 9.5 vesicles. The compressibility behavior and molecular area determination from Langmuir–Blodgett films differs between the two pH forms, which coupled to the thermal stability have led the authors to suggest that at pH 5.5 two di-cephalic imidazole surfactants chelate a single Cu(II), whereas at pH 9.5, Cu(II) bridges multiple surfactant ligands. Langmuir–Blodgett measurements at pH 9.5 show that an increase in headgroup area occurs in the presence of Cu(II). This increase in headgroup-area could result if the bis-imidazole headgroups lay flat in the bilayer plane such that they can be bridged by Cu(II) (Fig. 17). Increasing the di-imidazole headgroups in this way could explain why Cu(II) causes the formation of a curved, vesicle bilayer instead of a planar lipid bilayer [36]. Thus at pH 9.5 while the apo-dicephalic surfactant forms planar bilayers, in the presence of 0.5 equiv. of Cu(II), blue multilamellar vesicles form.

FF-TEM was utilized to study a similar planar-bilayer-to-vesicle transition which occurs upon addition of 2 equiv. of Cu(II) to the mono-imidazole amphiphile, dihexadecyl [5-(1-imidazolyl)-3-oxapentyl]-methylammonium chloride (Fig. 18) [37]. Spectrophotometric titration of the mono-imidazole amphiphile with Cu(II) indicates Cu(II) was coordinated as a 1:4 metal/ligand complex. As was the case with the dicephalic bis-imidazole ligand, 1,3-bis(1-imidazolyl)-2-propyl octadecanoate (Fig. 16), the titration data are also consistent with Cu(II) coordination by four equiv. of the

mono imidazole surfactant authors (Fig. 18). This coordination may force the imidazole groups to become more parallel to the bilayer plane, increasing the effective headgroup area and favoring a vesicle morphology over a planar lipid bilayer [10]. Imidazole forms 4:1 ligand/metal complexes with Cu(II) with a stability constant of β_4 of 9.6×10^{12} [16].

7. Amphiphilic 2,2′-bipyridine surfactants

A surfactant consisting of 2,2′-bipyridine appended by two lipophilic hydrocarbon chains (Fig. 19) forms vesicles upon complexation with Fe(II) [38,39] and other metals. These compounds have been reviewed recently, and thus are only mentioned here briefly. The cis-dicyano, bis 4-4′dinonyl-2,2′-bipyridine complex of Fe(II) forms vesicles ranging from 200 to 500 nm in diameter with an inner aqueous core, in which carboxyfluorescein has been trapped. The aggregate morphologies vary depending on the alkyl chain length. With C4–C5 alkyl chains, rod-shaped vesicles were formed that were 60–150 nm in diameter and 650–3500 nm long. The characteristic solvatochromism of $Fe(biby)_2(CN)_2$, which arises from hydrogen bonding of the CN^- ligands with protic solvents, is also evident in the self-assembled structures.
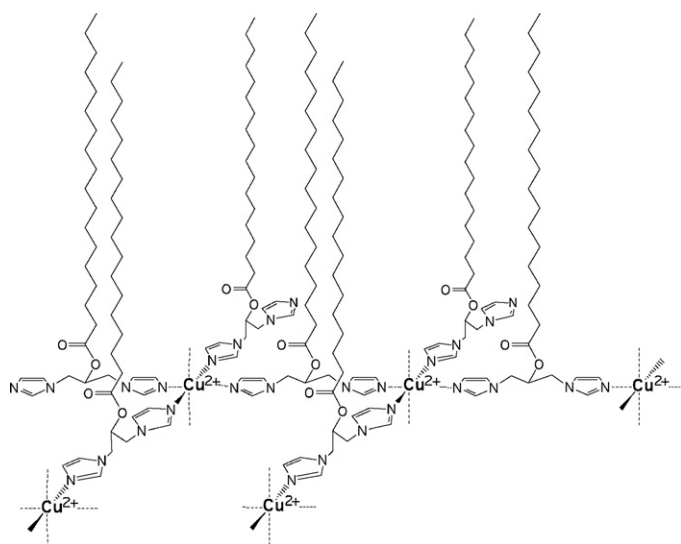

Fig. 17. Schematic of the proposed coordination of the Cu(II)-di-imidazole surfactant at pH 9.5 in a Langmuir–Blodgett monolayer (adapted from Ref. [36]; the square planar geometry at Cu(II) is not meant to be implied).
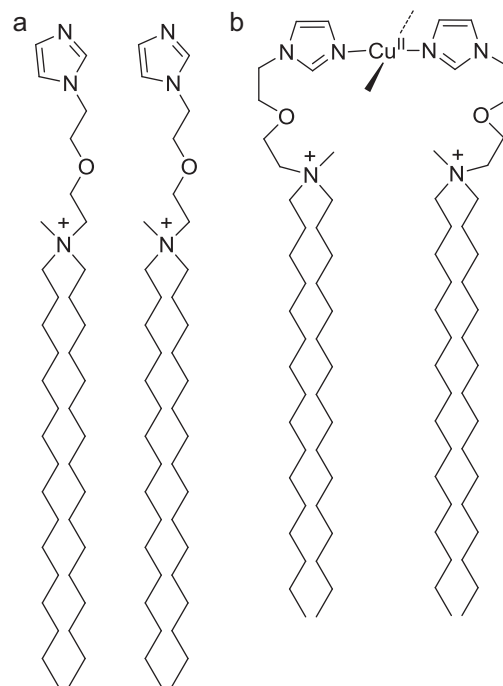

Fig. 18. Schematic of the conformation of the mono-imidazole surfactant, in (a) a metal-free planar bilayer and (b) in a vesicle bilayer after Cu(II) addition. In (b) two of the mono-imidazole surfactant molecules are omitted for clarity; adapted from Ref. [37].
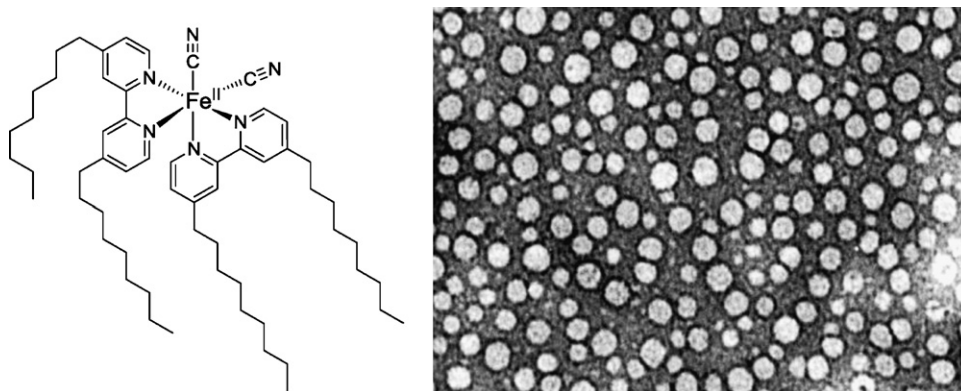
Fig. 19. Fe(II)(biby-{C9}$_2$)$_2$(CN)$_2$ (left) and TEM of vesicles of Fe(biby)$_2$(CN)$_2$ (right; reproduced with permission [38]).
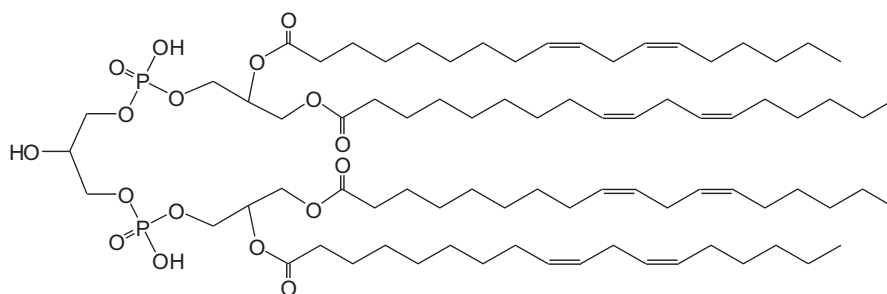

Fig. 20. A representative structure of a cardiolipin. The headgroup is conjugated to fatty acids of varying lengths and degrees of unsaturation.
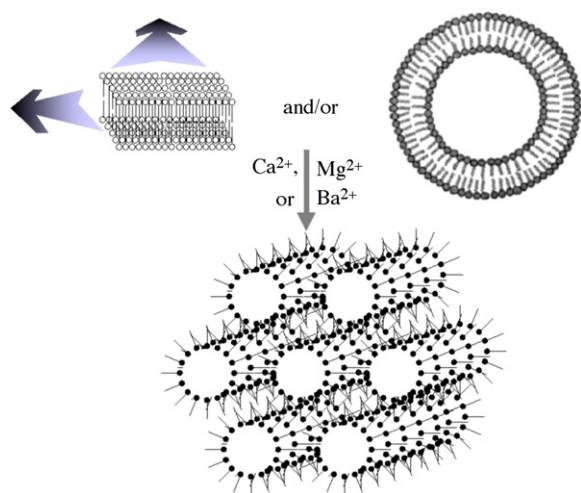

Fig. 21. Schematic of a dispersed bilayer to reversed hexagonal phase transition.

8. Cardiolipins

Metal-dependent phase behavior has been observed with many lipids, although most often the effects have been with the alkali metals as opposed to transition metal ions. Among phospholipids, one interesting class are the cardiolipins [40–43]. Cardiolipins are found in the inner membrane of mitochondria and are produced as a suite of phospholipids that consist of a biphosphatidyl glycerol headgroup conjugated to a variety of fatty acids (Fig. 20). Any given cardiolipin suite includes a mixture of saturated and unsaturated fatty acid tails that range in length from C14 to C18 [40–43].

FF-TEM images reveal that when dissolved in water, cardiolipin forms a dispersed bilayer phase (i.e., planar lipid bilayers or vesi-cles) and in the presence of Ba^{2+}, Ca^{2+}, Mg^{2+}, or Sr^{2+}, cardiolipin precipitates out of solution as a reversed hexagonal phase (Fig. 21) [42,43]. The temperature dependence of the lamellar to hexagonal transition is dependent on the metal cation involved. For example, in the presence of Ba^{2+} or Sr^{2+}, the transition only occurs at temperatures greater than 20–25 °C, however, Mg^{2+} or Ca^{2+} induce the transition at temperatures above 0 °C [43]. A cardiolipin mixture that contains a greater percentage of unsaturated lipids undergoes the phase transition at a lower temperature relative to a mixture with more saturated lipids [42]. The vesicle-to-hexagonal phase lipid transition can be reversed by the addition of EDTA [41].

While the self-assembly characteristics of the cardiolipins is not an example of a metal-induced micelle-to-vesicle transition, it seems likely that transition metals could well induce similar phase changes. Moreover, oxyanions of transition metals that interact with phosphates would be interesting to investigate. In addition these and other phospholipids provide a good scaffold for derivatization with various ligand moieties for future metal-induced self assembly investigations.

9. Summary

Naturally occurring, and synthetic surfactants exhibit metal-dependent phase behavior that can be rationalized in terms of how metal coordination by the surfactant headgroup affects the surfactant geometry. Understanding the interplay between surfactant self-assembly and coordination chemistry has the potential to produce new nanoscopic materials with metal-dependent physical properties and in particular through a controlled micelle-to-vesicle transition. Advances in the techniques used for studying such colloids (i.e., small-angle scattering, electron microscopy) holds promise to develop a greater understanding of the chemical principles that govern the biologically and technologically relevant field of metal-chelating surfactants.

Acknowledgements

References

[1] P.C. Griffiths, I.A. Fallis, T. Tatchell, L. Bushby, A. Beeby, Adv. Colloid Interface Sci. 144 (2008) 13.
[2] P.C. Griffiths, I.A. Fallis, T. Chuenpratoom, R. Watanesk, Adv. Colloid Interface Sci. A 122 (2006) 107.
[3] A. Accardo, D. Tesauro, L. Aloj, C. Pedone, G. Morelli, Coord. Chem. Rev. 253 (2009) 2193.
[4] F. Mancin, P. Scrimin, P. Tecilla, U. Tonellato, Coord. Chem. Rev. 253 (2009) 2150.
[5] J. Zhang, X.G. Meng, X.C. Zeng, X.Q. Yu, Coord. Chem. Rev. 253 (2009) 2166.
[6] P. Pallavicini, Y.A. Diaz-Fernandez, L. Pasotti, Coord. Chem. Rev. 253 (2009) 2226.
[7] M. Hebrant, Coord. Chem. Rev. 253 (2009) 2186.
[8] M.S. Goedheijt, B.E. Hanson, J.N.H. Reek, P.C.J. Kamer, P.W.N.M. van Leeuwen, J. Am. Chem. Soc. 122 (2000) 1650.
[9] A. Polyzos, A.B. Hughes, J.R. Christie, Langmuir 23 (2007) 1872.
[10] J.N. Israelachvili, D.J. Mitchell, B.W. Ninham, J. Chem. Soc. Faraday Trans. II 72 (1976) 1525.
[11] J.S. Martinez, G.P. Zhang, P.D. Holt, H.-T. Jung, C.J. Carrano, M.G. Haygood, A. Butler, Science 287 (2000) 1245.
[12] M. Sandy, A. Butler, Chem. Rev. 109 (2009) 4580.
[13] J.S. Martinez, A. Butler, J. Biol. Inorg. Chem. 101 (2007) 1692.
[14] T. Owen, R. Pynn, J.S. Martinez, A. Butler, Langmuir 21 (2005) 12109.
[15] T. Owen, R. Pynn, B. Hammouda, A. Butler, Langmuir 23 (2007) 9393.
[16] L.G. Sillén, A.E. Martell, Stability Constants of Metal-Ion Complexes. Supplement, Chemical Society, London, 1971, vol. 1, 2.
[17] T. Owen, S.M. Webb, A. Butler, Langmuir 24 (2008) 4999.
[18] J.S. Martinez, J.N. Carter-Franklin, E.L. Mann, J.D. Martin, M.G. Haygood, A. Butler, Proc. Natl. Acad. Sci. U.S.A. 100 (2003) 3754.
[19] J.D. Martin, Y. Ito, V.V. Homann, M.G. Haygood, A. Butler, J. Biol. Inorg. Chem. 11 (2006) 633.
[20] Y. Ito, A. Butler, Limnol. Oceanogr. 50 (2005) 1918.
[21] V.V. Homann, M. Sandy, J.A. Tincu, A.S. Templeton, B.M. Tebo, A. Butler, J. Natl. Prod. 72 (2009) 884.
[22] L.G. Sillén, A.E. Martell, J. Bjerrum, Stability Constants of Metal-Ion Complexes, xviii, Chemical Society, London, 1964, p. 754.
[23] L.D. Loomis, K.N. Raymond, Inorg. Chem. 30 (1991) 906.
[24] R.J. Abergel, J.A. Warner, D.K. Shuh, K.N. Raymond, J. Am. Chem. Soc. 128 (2006) 8920.
[25] S.M. Cohen, M. Meyer, K.N. Raymond, J. Am. Chem. Soc. 120 (1998) 6277.
[26] M. Apostol, P. Baret, G. Serratrice, J. Desbrieres, J.L. Putaux, M.J. Stebe, D. Expert, J.L. Pierre, Angew. Chem. Int. Ed. 44 (2005) 2580.
[27] L. Bednarova, J. Brandel, A.D. d'Hardemare, J. Bednar, G. Serratrice, J.L. Pierre, Chem. Eur. J. 14 (2008) 3680.
[28] J. Brandel, S. Torelli, G. Gellon, G. Serratrice, J.L. Putaux, J.L. Pierre, Eur. J. Inorg. Chem. (2009) 86.
[29] J.L. Pierre, A.D. d'Hardemare, G. Serratrice, S. Torelli, CR Chim. 10 (2007) 613.
[30] R. Lu, Y. Kamiya, T. Miyakoshi, Talanta 71 (2007) 1536.
[31] D. Mossialos, J.-M. Meyer, H. Budzikiewicz, U. Wolff, N. Koedam, C. Baysse, V. Anjaiah, P. Cornelis, Appl. Environ. Microbiol. 66 (2000) 487.
[32] X. Huang, M.W. Cao, J.B. Wang, Y.L. Wang, J. Phys. Chem. B 110 (2006) 19479.
[33] X.Z. Luo, S.X. Wu, Y.Q. Liang, Chem. Commun. (2002) 492.
[34] X.Z. Luo, W.G. Miao, S.X. Wu, Y.Q. Liang, Langmuir 18 (2002) 9611.
[35] G. Wang, G. Li, Tenside Surfact. Det. 47 (2010) 258.
[36] N.A.J.M. Sommerdijk, K.J. Booy, A.M.A. Pistorius, M.C. Feiters, R.J.M. Nolte, B. Zwanenburg, Langmuir 15 (1999) 7008.
[37] J.H. Van Esch, A.L.H. Stols, R.J.M. Nolte, J. Chem. Soc. Chem. Commun. (1990) 1658.
[38] P. Garcia, J. Marques, E. Pereira, P. Gameiro, R. Salema, B. de Castro, Chem. Commun. (2001) 1298.
[39] P. Garcia, P. Eaton, H.P.M. Geurts, M. Sousa, P. Gameiro, M.C. Feiters, R.J.M. Nolte, E. Pereira, B. de Castro, Langmuir 23 (2007) 7951.
[40] R.P. Rand, S. Sengupta, Biochim. Biophys. Acta 225 (1972) 484.
[41] W.J. Vail, J.G. Stollery, Biochim. Biophys. Acta 551 (1979) 74–84.
[42] I. Vasilenko, B. Dekruijff, A.J. Verkleij, Biochim. Biophys. Acta 684 (1982) 282–286.
[43] A. Ortiz, J.A. Killian, A.J. Verkleij, J. Wilschut, Biophys. J. 77 (1999) 2003.